Hindawi
Mathematical Problems in Engineering
Volume 2018, Article ID 4968682, 11 pages
https://doi.org/10.1155/2018/4968682

Research Article

Efficient Impulsive Noise Mitigation for OFDM Systems Using the Alternating Direction Method of Multipliers

Xin-Rong Lv,[1,2] **Youming Li**,[1] **and Yu-Cheng He**[3]

[1] *The Faculty of Information Science and Engineering, Ningbo University 315211, China*
[2] *The School of Intelligent Electronics, Zhejiang Business Technology Institute, Ningbo 315012, China*
[3] *The College of Information Science and Engineering, National Huaqiao University, Xiamen 361021, China*

Correspondence should be addressed to Youming Li; liyouming@nbu.edu.cn

Received 24 January 2018; Accepted 2 May 2018; Published 7 June 2018

Academic Editor: Paolo Addesso

An efficient impulsive noise estimation algorithm based on alternating direction method of multipliers (ADMM) is proposed for OFDM systems using quadrature amplitude modulation (QAM). Firstly, we adopt the compressed sensing (CS) method based on the ℓ^1-norm optimization to estimate impulsive noise. Instead of the conventional methods that exploit only the received signal in null tones as constraint, we add the received signal of data tones and QAM constellations as constraints. Then a relaxation approach is introduced to convert the discrete constellations to the convex box constraints. After that a linear programming is used to solve the optimization problem. Finally, a framework of ADMM is developed to solve the problem in order to reduce the computation complexity. Simulation results for 4-QAM and 16-QAM demonstrate the practical advantages of the proposed algorithm over the other algorithms in bit error rate performance gains.

1. Introduction

Power line communications (PLC) have become an attractive communication solution for smart grid and other applications due to their advantages of high penetration and low deployment costs over other communication technologies [1–3]. The applications of PLC, however, are limited by some unfavorable factors, among which the impulsive noise (IN) is the major factor that influences the data transmission over power grid. Impulsive noise can be divided roughly into two categories: asynchronous and periodic [4]. Asynchronous impulsive noise is primarily caused by switching transients of electrical appliances and characterized by short duration and high power impulses with random arrivals. Periodic impulsive noise typically arises from switching mode power supplies and contains longer bursts of interference spikes that occur periodically with half the main cycle of grid.

Orthogonal frequency-division multiplexing (OFDM) is less sensitive to impulsive noise than single carrier by spreading the effect of impulsive noise across all subcarriers [5]. Thus, OFDM has found applications in the physical layer technology by most modern PLC standards. Recent field measurements, however, have identified that the power spectral density (PSD) of impulsive noise can exceed that of background noise by at least 20 dB or even 50 dB in some scenarios [6, 7]. Conventional OFDM-based PLC systems can deteriorate sharply in the presence of impulsive noise.

In this work, we focus on the mitigation of asynchronous impulsive noise, for which the common methods include clipping or blanking [8–11]. In [8, 9], the optimal clipping and blanking thresholds are derived in closed-form under the conditions that the occurrence probability of impulsive noise and the noise power can be perfectly estimated at the receiver. In [10], the method of moments (MoM) is used to estimate the parameters and update adaptively the thresholds on assuming that the statistics of impulsive noise maintains stationary in a long period. In [11], a framework of optimal blanking threshold (OBT) estimation is proposed based on the peak-to-average power ratio (PAPR) of signals. However it is difficult to obtain the PAPR values at the receiver. In [12], an MMSE estimator is proposed on the assumption that the impulsive noise is i.i.d. in the time domain, which yields an

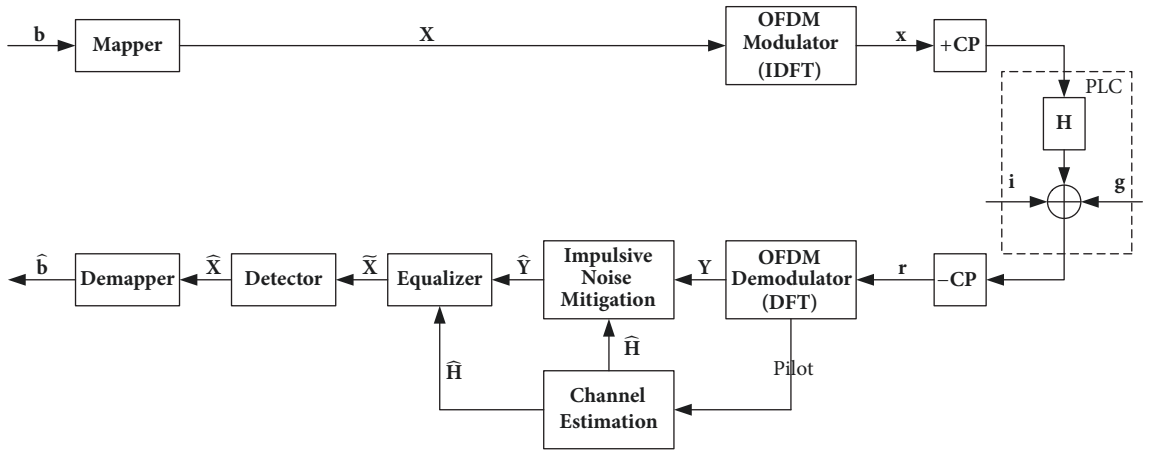

Figure 1: PLC system block diagram.

approximate optimal estimation only when the noise state information (NSI) is known.

Note that the above methods need to estimate the parameters of either impulsive noise or OFDM signal. Since the impulsive noise in the PLC environments is time-varying, accurate estimation of the parameters can be an exhausting task. To avoid impractical parameter estimation, nonparametric mitigation methods may be preferred. In [13], the compressed sensing (CS) is applied in the mitigation with observing that the asynchronous impulsive noise is sparse in the time domain; that is, the number of impulses in an OFDM symbol cannot exceed some threshold. In [14], the CS-based technique is extended to the scenarios of bursty impulsive noise. Due to the sparsity property of impulsive noise, it can also be recovered by the Sparse Bayesian Learning (SBL) algorithm [15]. Moreover, in [15], two enhanced SBL algorithms for impulsive noise mitigation are proposed: SBL using all tones and SBL using decision feedback. These SBL algorithms can improve the performance and robustness of mitigation by incorporating some a priori information on the impulsive noise, but at fairly high complexities. In [16], the orthogonal clustering (OC) algorithm is developed to find the dominant support of asynchronous IN, and then the MMSE estimate of IN is derived. With the advantage of low complexity, it needs some correct parameter information about IN and the background noise variance at the same time.

In this paper, we investigate the CS technique for asynchronous impulsive noise mitigation in OFDM-based PLC systems with QAM by exploiting the modulus property of QAM constellations. First, we adopt the CS algorithm based on the ℓ^1-norm minimization to estimate the impulsive noise with the constraint on the projection of impulsive noise onto null tones. Then, we add the received signal of data tones and source QAM symbols as constraints. As a result, we obtain a nonconvex optimization problem based on the ℓ^1-norm minimization with constraints on the information of all tones of OFDM symbols. Next, we convert the nonconvex problem into a linear programming (LP) problem with proper relaxation. In order to reduce the computational complexity, we introduce the ADMM framework to solve the LP optimization problem. Consequently, we obtain an IN estimation algorithm based on ADMM which is able to exploit the information with respect to all tones. With independence of channel coding, the proposed algorithm is suitable for both uncoded and coded PLC systems. In computer simulations, we use a rate-1/2 convolutional code for the coded systems and consider two models for generating the impulsive noise. The main novel contributions of this paper are tripartite: (1) both the received signal of all tones and source QAM symbols property are exploited to improve the IN estimation performance, which has not been reported in the literature. (2) A relaxation approach is introduced to convert the discrete QAM constellations into convex set, which makes a nonconvex optimization problem become a convex optimization problem. (3) An ADMM framework is developed to solve the resulting optimization problem, which can obtain the same performance as the LP algorithm but has lower computation complexity than the LP algorithm.

The remainder of this paper is organized as follows. In Section 2, the system model and the impulsive noise models are briefly described. In Section 3, we first briefly introduce the CS algorithm with null tones using the system model and then derive a nonparametric algorithm by extending the CS algorithm to include all the tones. Furthermore, we derive a nonconvex optimization problem and approximate it into a standard LP problem. In Section 4, we propose an ADMM framework to solve the convex optimization problem. In Section 5, simulation results show the advantages of the proposed method in the error performance over a wide range of signal-to-noise ratio (SNR) values. Finally, Section 6 concludes the paper.

2. System Model

The complex baseband model for OFDM-based PLC systems is shown in Figure 1. At the transmitter, the frequency-domain OFDM symbols are mapped from the data bits and denoted in the vector form as $\mathbf{X} = (X_0, X_1, \ldots, X_N)^T$, where N is the total number of subcarriers. The OFDM modulator, as an inverse discrete Fourier transformation

(IDFT), converts the frequency-domain OFDM symbols to the time-domain OFDM signals $\mathbf{x} = (x_0, x_1, \ldots, x_N)^T$ as follows:

$$\mathbf{x} = \mathbf{F}^* \mathbf{X}, \tag{1}$$

where $\mathbf{F}$ is an N point DFT matrix and $\mathbf{F}^*$ is the Hermitian transpose of $\mathbf{F}$. Then, a cyclic prefix (CP) of length larger than the channel delay spread is inserted ahead of $\mathbf{x}$ for circumventing the intersymbol interference (ISI) over the PLC channel.

Noise in the PLC channel cannot be considered simply as a stationary AWGN, but may be viewed as an additive mixture of the background AWGN and the impulsive noise. It is known that asynchronous impulsive noise is time-variant with a short duration, random occurrence, and a high power spectral density. Thus, at the receiver, the received time-domain OFDM signals with the CP dropped can be expressed by

$$\mathbf{r} = \mathbf{H}\mathbf{x} + \mathbf{i} + \mathbf{g}, \tag{2}$$

where $\mathbf{H}$ is an $N \times N$ circulant matrix whose first column is formed by the zero-padded channel impulse response, $\mathbf{i}$ represents the impulsive noise vector, $\mathbf{g}$ represents the background noise vector of N i.i.d. AWGN variables, and the vectors $\mathbf{r}$, $\mathbf{x}$, $\mathbf{i}$, and $\mathbf{g}$ in the time domain are all located in the N-dimensional complex signal space $\mathbb{C}^N$.

Through the OFDM demodulator, the received signal vector $\mathbf{r}$ in the time domain is converted by DFT into the frequency domain as

$$\mathbf{Y} = \mathbf{F}\mathbf{r} = \mathbf{F}\mathbf{H}\mathbf{F}^*\mathbf{X} + \mathbf{F}\mathbf{i} + \mathbf{F}\mathbf{g} = \mathbf{\Lambda}\mathbf{X} + \mathbf{F}\mathbf{i} + \mathbf{G}, \tag{3}$$

where $\mathbf{\Lambda} = \mathbf{F}\mathbf{H}\mathbf{F}^* = \mathrm{diag}(H_0, H_1, \ldots, H_{N-1})$ is a diagonal matrix with diagonal elements H_i being the point DFT coefficients of channel impulse response. $\mathbf{G} = \mathbf{F}\mathbf{g}$ is the DFT of $\mathbf{g}$, which can also be assumed to be AWGN since $\mathbf{F}$ is an unitary matrix.

Subsequently, the impulsive noise $\mathbf{i}$ is estimated and removed through the impulsive noise mitigation module, the channel distortion with respect to $\mathbf{\Lambda}$ can be compensated using a simple one-tap frequency-domain equalizer (FEQ), and the detector works as if only AWGN were present. Finally, the data bits are obtained by demapper.

In computer simulations, we consider two models for generating the impulsive noise components, respectively, Gaussian mixture (GM) model and Middleton Class A (MCA) noise model, which are widely used in PLC [17]. In the GM model, the probability density function (PDF) of a noise sample x is a weighted summation of K different Gaussian variables given by

$$f(x) = \sum_{k=0}^{K-1} p_k g_k(x), \tag{4}$$

where $g_k(x)$ is the PDF of the complex Gaussian variable with zero-mean and variance γ_k and p_k is the mixing probability of the kth component such that $\sum_{k=0}^{K-1} p_k = 1$.

In the MCA noise model, the PDF of the noise sample x is given in a different form:

$$f(x) = \sum_{k=0}^{\infty} \pi_k g_k(x), \tag{5}$$

where π_k is the mixing probability subject to the Poisson distribution with parameter A, i.e., $\pi_k = e^{-A}A^k/k!$ for $k = 0, 1, \ldots$. The MCA model can be viewed as a special case of the GM model with $p_k = \pi_k$ and an infinite number of Gaussian components with zero-mean and variance:

$$\gamma_k = \frac{k/A + \Gamma}{1 + \Gamma}, \tag{6}$$

where $k = 0, 1, \ldots, K$, the parameter A denotes the impulsive index, and Γ is the mean power ratio of background-to-impulsive noises [15].

3. The IN Estimation Using LP

In OFDM-based PLC systems, N subcarriers of an OFDM symbol can be divided into two parts: null tones and data tones. The null tones are occupied by means of setting the all-zero input and the data tones are used to transmit data symbols or pilot symbols.

3.1. The IN Estimation with Null Tones. Let $\overline{D}$ denote the index set of null tones with a total number M. Let $(\cdot)$ denote the operation of forming a submatrix (or subvector) by selecting the rows (or elements) indexed by D. According to the arrangement of tone clusters, the received OFDM symbols at the null tones are obtained from (3) as

$$\mathbf{Y}_{\overline{D}} = (\mathbf{\Lambda}\mathbf{X})_{\overline{D}} + \mathbf{F}_{\overline{D}}\mathbf{i} + \mathbf{G}_{\overline{D}}, \tag{7}$$

where $\mathbf{G}_{\overline{D}} \sim \mathcal{CN}(\mathbf{0}, \sigma^2\mathbf{I}_M)$ is a complex AWGN vector with zero-mean and variance matrix $\sigma^2\mathbf{I}_M$.

With known zero symbols $\{X_i,\ i \in \overline{D}\}$ at the null tones, (7) becomes

$$\mathbf{Y}_{\overline{D}} = \mathbf{F}_{\overline{D}}\mathbf{i} + \mathbf{G}_{\overline{D}}, \tag{8}$$

which is a group of linear observations of the impulsive noise. Notice that the matrix $\mathbf{F}_{\overline{D}}$ is underdetermined since $M \ll N$. Thus, (8) can also be viewed as underdetermined equations with measurement noise. It is generally accepted that the asynchronous impulsive noise is sparse in the time domain [13–15]. Thus, the CS technique can be employed to estimate the impulsive noise $\mathbf{i}$ according to (8) [13]. Using the minimum ℓ^1-norm reconstruction algorithm for CS [18], we can formulate the impulsive noise estimation as the following convex optimization problem:

$$\begin{aligned} \min \quad & \|\mathbf{i}\|_1 \\ \text{s.t.} \quad & \left\|\mathbf{Y}_{\overline{D}} - \mathbf{F}_{\overline{D}}\mathbf{i}\right\|_2^2 \le \varepsilon_1, \end{aligned} \tag{9}$$

where $\varepsilon_1 > 0$ is the maximum tolerable root-mean-square error (RMSE) due to the background noise and $\|\mathbf{i}\|_p$ denotes

the ℓ^p-norm for a real number $p \geq 1$ that is given by $\|\mathbf{i}\|_p = (\sum_{k=1}^{n} |i_k|^p)^{1/p}$.

Let $\widehat{\mathbf{i}}$ be a solution to the problem in (9). The impacts of the impulsive noise can be removed by subtraction as follows:

$$\widehat{\mathbf{Y}} \triangleq \mathbf{Y} - \mathbf{F}\widehat{\mathbf{i}} = \mathbf{\Lambda X} + \mathbf{F}\left(\mathbf{i} - \widehat{\mathbf{i}}\right) + \mathbf{G}. \tag{10}$$

Assuming the impulsive noise residual $(\mathbf{i}-\widehat{\mathbf{i}})$ can be negligible, the receiver can then proceed as if only Gaussian noise is present and apply the conventional zero-forcing equalization algorithm.

3.2. The IN Estimation with All Tones. It is known that increasing the number of null-data tones is equivalent to increasing the rank of matrix $\mathbf{F}_{\overline{D}}$ in (9), which can promote the accuracy of impulsive noise estimation. However, the improvement will be obtained at a cost of losing system throughput. To avoid this loss, we should not increase the number of non-data tones, but resort to exploiting the information of data tones for the purpose of improving the impulsive noise estimation.

Some modern PLC standards, such as G.hnem [19], adopt QAM modulation which requires a coherent receiver. Many simulation results have shown that the coherent receiver can significantly increase system performance even in scenarios with strong impulsive noise and time-varying channel behavior [19]. Let Ω be the set of QAM constellation points. Exploiting the information of data tones, we can formulate a new impulsive noise estimation optimization problem:

$$\begin{aligned} \min \quad & \|\mathbf{i}\|_1 \\ \text{s.t.} \quad & \left\|\mathbf{Y}_{\overline{D}} - \mathbf{F}_{\overline{D}}\mathbf{i}\right\|_2^2 \leq \varepsilon_1 \\ & \left\|\mathbf{Y}_D - (\mathbf{\Lambda X})_D - \mathbf{F}_D\mathbf{i}\right\|_2^2 \leq \varepsilon_2 \\ & X_k \in \Omega, \quad \forall k \in D, \end{aligned} \tag{11}$$

where D denotes the index set of data tones with a total number $N - M$. Compared with (9), (11) adds some new constraints corresponding to the information of data tones.

Defining a new vector $\mathbf{t} = [\mathbf{X}^T\ \mathbf{i}^T]^T \in \mathbb{C}^{2N}$, the source symbol vector $\mathbf{X}$ and the impulsive noise vector $\mathbf{i}$ can be expressed as

$$\begin{aligned} \mathbf{X} &= \mathbf{U}\mathbf{t} \\ \mathbf{i} &= \mathbf{V}\mathbf{t}, \end{aligned} \tag{12}$$

where the matrix $\mathbf{U} \triangleq [\mathbf{I}_N\ \mathbf{0}_N] \in \mathbb{R}^{N\times 2N}$, $\mathbf{V} \triangleq [\mathbf{0}_N\ \mathbf{I}_N] \in \mathbb{R}^{N\times 2N}$. We use $\mathbf{0}_N$ to denote the $N \times N$ zero matrix and $\mathbf{I}_N$ to denote the $N \times N$ identity matrix. Then (11) can be rewritten as

$$\begin{aligned} \min \quad & \|\mathbf{Vt}\|_1 \\ \text{s.t.} \quad & \left\|\mathbf{Y}_{\overline{D}} - \mathbf{F}_{\overline{D}}\mathbf{Vt}\right\|_2^2 \leq \varepsilon_1 \\ & \left\|\mathbf{Y}_D - \mathbf{\Phi t}\right\|_2^2 \leq \varepsilon_2 \\ & \mathbf{Ut}\,(k) \in \Omega, \quad \forall k \in D, \end{aligned} \tag{13}$$

where $\mathbf{\Phi} \triangleq [\mathbf{\Lambda}_D\ \mathbf{F}_D]$. Clearly, the optimization problem in (13) belongs to the class of NP-hard problems because there is a discrete constraint [20]. To make the optimization problem feasible, we convert the nonconvex constraint into a convex constraint in the sequel.

We use $\Omega_{\mathrm{Re}} = \mathrm{Re}(\Omega)$ and $\Omega_{\mathrm{Im}} = \mathrm{Im}(\Omega)$ to represent, respectively, the sets of real and imaginary coordinates of the set Ω. According to the origin-symmetric property of Ω, the constellation covers a rectangular region with boundaries given by

$$\begin{aligned} |\mathrm{Re}\,(S)| &\leq \max\{a \in \Omega_{\mathrm{Re}}\} \triangleq u_R, \quad \forall S \in \Omega \\ |\mathrm{Im}\,(S)| &\leq \max\{a \in \Omega_{\mathrm{Im}}\} \triangleq u_I, \quad \forall S \in \Omega, \end{aligned} \tag{14}$$

where $u_R = u_I$ holds for square QAM constellations.

Substituting (14) into (13), the nonconvex constraint is relaxed to the convex box constraint (15):

$$\begin{aligned} -u_R &\leq \mathrm{Re}\,(\mathbf{Ut}\,(k)) \leq u_R \\ -u_I &\leq \mathrm{Im}\,(\mathbf{Ut}\,(k)) \leq u_I. \end{aligned} \tag{15}$$

Consequently, we obtain the following convex problem:

$$\begin{aligned} \min \quad & \|\mathbf{Vt}\|_1 \\ \text{s.t.} \quad & \left\|\mathbf{Y}_{\overline{D}} - \mathbf{F}_{\overline{D}}\mathbf{Vt}\right\|_2^2 \leq \varepsilon_1 \\ & \left\|\mathbf{Y}_D - \mathbf{\Phi t}\right\|_2^2 \leq \varepsilon_2 \\ & -u_R \cdot \mathbf{1}_N \preceq \mathrm{Re}\,(\mathbf{Ut}) \preceq u_R \cdot \mathbf{1}_N \\ & -u_I \cdot \mathbf{1}_N \preceq \mathrm{Im}\,(\mathbf{Ut}) \preceq u_I \cdot \mathbf{1}_N. \end{aligned} \tag{16}$$

$\mathbf{1}_N$ denotes the $N \times 1$ column vector with all elements being one.

In problems (9) and (16), it is not easy to choose the constants ε_1 and ε_2 that are dependent on the noise power estimation. Recalling (2) for the received OFDM signals, we denote the sum of impulsive noise and background noise as $\mathbf{e} = \mathbf{i} + \mathbf{g}$. In reality the amplitudes of asynchronous impulsive noise samples are much larger than those of background noise samples. So it is reasonable to consider $\|\mathbf{e}\|_1$ as an approximation to $\|\mathbf{i}\|_1$ with $\mathbf{g}$ omitted such that the constants ε_1 and ε_2 diminish in (9) and (16). Upon replacing $\|\mathbf{i}\|_1$ by $\|\mathbf{e}\|_1$ we can rewrite the problem (16) as

$$\begin{aligned} \min \quad & \|\mathbf{Vt}\|_1 \\ \text{s.t.} \quad & \mathbf{Y} = \mathbf{At} \\ & -u_R \cdot \mathbf{1}_N \preceq \mathrm{Re}\,(\mathbf{Ut}) \preceq u_R \cdot \mathbf{1}_N \\ & -u_I \cdot \mathbf{1}_N \preceq \mathrm{Im}\,(\mathbf{Ut}) \preceq u_I \cdot \mathbf{1}_N, \end{aligned} \tag{17}$$

where

$$\begin{aligned} \mathbf{t} &= \left[\mathbf{X}^T\ \ \mathbf{e}^T\right]^T \\ \mathbf{Y} &= \left[\mathbf{Y}_{\overline{D}}^T\ \ \mathbf{Y}_D^T\right]^T \\ \mathbf{A} &= \begin{bmatrix} \mathbf{F}_{\overline{D}}\mathbf{V} \\ \mathbf{\Phi} \end{bmatrix}. \end{aligned} \tag{18}$$

It can verify that problem (17) is a typical linear programming (LP) problems, which can be solved by using the on-the-shelf software packages such as CVX [21]. We refer to the algorithm as "LP-All".

4. The IN Estimation Using ADMM

Although in general the above LP-based approaches can provide satisfying results, they become computationally demanding as the signal dimension increases because of matrix inversion [22]. In this section, we propose the ADMM framework to solve the IN estimation optimization problems.

4.1. Framework of ADMM. Let us consider the optimization problem in the following form [23]:

$$\begin{aligned} \min \quad & f(x) + g(z) \\ \text{s.t.} \quad & Ax + Bz = c \end{aligned} \tag{19}$$

with variable $x \in \mathbb{R}^n$ and $z \in \mathbb{R}^m$, where $A \in \mathbb{R}^{p\times n}$, $B \in \mathbb{R}^{p\times m}$, and $c \in \mathbb{R}^p$. We also assume that f and g are convex functions. The augmented Lagrangian function of the problem (19) is given by

$$\begin{aligned} \mathscr{L}(x, \lambda, z) = {} & f(x) + g(z) + \lambda^T (Ax + Bz - c) \\ & + \frac{\rho}{2} \|Ax + Bz - c\|_2^2, \end{aligned} \tag{20}$$

where $\lambda \in \mathbb{R}^p$ is the Lagrangian multiplier and $\rho > 0$ is a penalty parameter. Given (z^k, λ^k), ADMM consists of the iterations as follows:

$$\begin{aligned} x^{k+1} &\longleftarrow \operatorname*{argmin}_x \mathscr{L}\left(x, z^k, \lambda^k\right) \\ z^{k+1} &\longleftarrow \operatorname*{argmin}_z \mathscr{L}\left(x^{k+1}, z, \lambda^k\right) \\ \lambda^{k+1} &\longleftarrow \lambda^k + \rho\left(Ax^{k+1} + Bz^{k+1} - c\right). \end{aligned} \tag{21}$$

Defining the scaled dual variable $u = (1/\rho)\lambda$, we can express ADMM iterations as

$$\begin{aligned} x^{k+1} &\longleftarrow \operatorname*{argmin}_x \left(f(x) + \frac{\rho}{2}\left\|Ax + Bz^k - c + u^k\right\|_2^2\right) \\ z^{k+1} &\longleftarrow \operatorname*{argmin}_z \left(g(z) + \frac{\rho}{2}\left\|Ax^{k+1} + Bz - c + u^k\right\|_2^2\right) \\ u^{k+1} &\longleftarrow u^k + Ax^{k+1} + Bz^{k+1} - c. \end{aligned} \tag{22}$$

ADMM is proved to converge for all positive values of ρ under quite mild conditions, which makes the selection of ρ rather flexible [24]. Hence, we can simply use a fixed positive constant for $\rho = 1$ in our work.

4.2. The IN Estimation with All Tones Using ADMM (ADMM-All). In ADMM form, the IN estimation algorithm (17) can be written as

$$\begin{aligned} \min \quad & \mathscr{I}(\mathbf{t}) + \mathscr{G}(\mathbf{z}_1) + \|\mathbf{z}_2\|_1 \\ \text{s.t.} \quad & \mathbf{U}\mathbf{t} - \mathbf{z}_1 = \mathbf{0} \\ & \mathbf{V}\mathbf{t} - \mathbf{z}_2 = \mathbf{0}, \end{aligned} \tag{23}$$

where $\mathscr{I}(\mathbf{t})$ is the indicator function of equality constrains and $\mathscr{G}(\mathbf{z}_1)$ is the indicator function of the box constraint of (17).

We introduce an auxiliary vector $\mathbf{z} = [\mathbf{z}_1^T\ \mathbf{z}_2^T]^T \in \mathbb{C}^{2N}$ with $\mathbf{z}_1 = \mathbf{U}\mathbf{z}$ and $\mathbf{z}_2 = \mathbf{V}\mathbf{z}$. Then the two constraints $\mathbf{U}\mathbf{t} - \mathbf{z}_1 = \mathbf{0}$ and $\mathbf{V}\mathbf{t} - \mathbf{z}_2 = \mathbf{0}$ can be combined into one constraint $\mathbf{t} - \mathbf{z} = \mathbf{0}$. So we can express the augmented Lagrangian function as follows:

$$\begin{aligned} \mathscr{L}(\mathbf{t}, \mathbf{z}, \lambda) = {} & \mathscr{I}(\mathbf{t}) + \mathscr{G}(\mathbf{U}\mathbf{z}) + \|\mathbf{V}\mathbf{z}\|_1 + \lambda^T(\mathbf{t} - \mathbf{z}) \\ & + \frac{\rho}{2}\|\mathbf{t} - \mathbf{z}\|_2^2. \end{aligned} \tag{24}$$

The corresponding ADMM iterations consisted of

$$\mathbf{t}^{k+1} \longleftarrow \prod\left(\mathbf{z}^k - \mathbf{u}^k\right) \tag{25}$$

$$\mathbf{z}_1^{k+1} \longleftarrow \mathscr{P}\left(\mathbf{U}\left(\mathbf{t}^{k+1} + \mathbf{u}^k\right)\right) \tag{26}$$

$$\mathbf{z}_2^{k+1} \longleftarrow \mathscr{S}_{1/\rho}\left(\mathbf{V}\left(\mathbf{t}^{k+1} + \mathbf{u}^k\right)\right) \tag{27}$$

$$\mathbf{u}^{k+1} \longleftarrow \mathbf{u}^k + \mathbf{t}^{k+1} - \mathbf{z}^{k+1}, \tag{28}$$

where $\prod$ is projection onto $\{\mathbf{t} \mid \mathbf{A}\mathbf{t} = \mathbf{Y}\}$ and $\mathscr{P}$ is Euclidian projection onto the box constraint (15).

The $\mathbf{t}$-update (25) involves solving a linearly constrained minimum Euclidean norm problem, which can be expressed as

$$\begin{aligned} \min_{\mathbf{t}} \quad & \left\|\mathbf{t} - \left(\mathbf{z}^k - \mathbf{u}^k\right)\right\|_2^2 \\ \text{s.t.} \quad & \mathbf{A}\mathbf{t} = \mathbf{Y}. \end{aligned} \tag{29}$$

The KKT (Karush-Kuhn-Tucker) conditions [22] for this problem are

$$\begin{bmatrix} \mathbf{I} & \mathbf{A}^T \\ \mathbf{A} & \mathbf{0} \end{bmatrix} \begin{bmatrix} \mathbf{t}^* \\ \nu^* \end{bmatrix} = \begin{bmatrix} \mathbf{z}^k - \mathbf{u}^k \\ \mathbf{Y} \end{bmatrix}, \tag{30}$$

where ν^* is the optimal dual variable. The solution $\mathbf{t}^*$ of the above equations is

$$\begin{aligned} \mathbf{t}^* = {} & \left(\mathbf{I} - \mathbf{A}^T\left(\mathbf{A}\mathbf{A}^T\right)^{-1}\mathbf{A}\right)\left(\mathbf{z}^k - \mathbf{u}^k\right) \\ & + \mathbf{A}^T\left(\mathbf{A}\mathbf{A}^T\right)^{-1}\mathbf{Y}. \end{aligned} \tag{31}$$

In $\mathbf{z}_1$-update (26), the $\mathscr{P}$ is elementwise Euclidian projection onto the box constraint (15), which is defined as

$$\mathscr{P}(a) = \begin{cases} u_R, & a > u_R \\ a, & |a| \le u_R \\ -u_R, & a < -u_R. \end{cases} \tag{32}$$

In $\mathbf{z}_2$-update (27), $\mathscr{S}_{1/\rho}(\mathbf{x}^{k+1} + \mathbf{u}^k)$ is the well-known elementwise soft thresholding operator [23], which is defined as

$$\mathscr{S}_\kappa(a) = \begin{cases} a - \kappa, & a > \kappa \\ 0, & |a| \le \kappa \\ a + \kappa, & a < -\kappa. \end{cases} \tag{33}$$

4.3. The IN Estimation with Null Tones Using ADMM (ADMM-Null). We first recast problem (9) as LP form:

$$\begin{aligned} \min \quad & \|\mathbf{e}\|_1 \\ \text{s.t.} \quad & \mathbf{Y}_{\overline{D}} = \mathbf{F}_{\overline{D}}\mathbf{e}. \end{aligned} \tag{34}$$

And then (34), named "LP-Null", can be written as

$$\begin{aligned} \min \quad & \mathcal{I}(\mathbf{e}) + \|\mathbf{z}\|_1 \\ \text{s.t.} \quad & \mathbf{e} - \mathbf{z} = \mathbf{0}, \end{aligned} \tag{35}$$

where $\mathcal{I}(\mathbf{e})$ is the indicator function of $\{\mathbf{e} \in \mathbb{C}^N \mid \mathbf{F}_{\overline{D}}\mathbf{e} = \mathbf{Y}_{\overline{D}}\}$. The augmented Lagrangian function of problem (35) is

$$\mathcal{L}(\mathbf{e}, \mathbf{z}, \lambda) = \mathcal{I}(\mathbf{e}) + \|\mathbf{z}\|_1 + \lambda^T(\mathbf{e} - \mathbf{z}) + \frac{\rho}{2}\|\mathbf{e} - \mathbf{z}\|_2^2. \tag{36}$$

According the ADMM iterations (22), we can obtain the update primal variables $\mathbf{e}$, $\mathbf{z}$, and a dual variable $\mathbf{u}$ as follows:

$$\mathbf{e}^{k+1} \longleftarrow \prod\left(\mathbf{z}^k - \mathbf{u}^k\right) \tag{37}$$

$$\mathbf{z}^{k+1} \longleftarrow \mathcal{S}_{1/\rho}\left(\mathbf{x}^{k+1} + \mathbf{u}^k\right) \tag{38}$$

$$\mathbf{u}^{k+1} \longleftarrow \mathbf{u}^k + \mathbf{x}^{k+1} - \mathbf{z}^{k+1}, \tag{39}$$

where $\prod$ is projection onto $\{\mathbf{e} \in \mathbb{C}^N \mid \mathbf{F}_{\overline{D}}\mathbf{e} = \mathbf{Y}_{\overline{D}}\}$ and $\mathcal{S}_{1/\rho}$ is the elementwise soft thresholding operator.

The solution of $\mathbf{e}$-update (37) can be derived using the similar method in (29)~(31) as follows:

$$\begin{aligned} \mathbf{e}^* = & \left(\mathbf{I} - \mathbf{F}_{\overline{D}}^T\left(\mathbf{F}_{\overline{D}}\mathbf{F}_{\overline{D}}^T\right)^{-1}\mathbf{F}_{\overline{D}}\right)\left(\mathbf{z}^k - \mathbf{u}^k\right) \\ & + \mathbf{F}_{\overline{D}}^T\left(\mathbf{F}_{\overline{D}}\mathbf{F}_{\overline{D}}^T\right)^{-1}\mathbf{Y}_{\overline{D}}. \end{aligned} \tag{40}$$

4.4. Complexity Analysis. The worst-case complexity of solving LP-Null and LP-All is $\mathcal{O}(N^3)$ by using the interior point method [22]. For the proposed ADMM-Null and ADMM-All algorithms, the leading computation cost is the matrix inversions and matrix multiplications in (40) and (31). However we notice that these inverses only have to be computed once. We can caching the matrix inversion and use this cached value in subsequent steps. The resulting complexity is $\mathcal{O}(N^2) + M^3$ for ADMM-Null and $\mathcal{O}(N^2) + N^3$ for ADMM-All. So the computation complexity of the IN estimation algorithm using ADMM is significantly lower than that using LP.

5. Simulation Results

In this section, we present computer simulation results for the proposed impulsive noise mitigation method in the complex baseband OFDM-based PLC systems over an ideal (unit-gain nonfading) channel and a 15-path multipath power line channel model [25], respectively. In our simulations, the impulsive noise samples are generated using the GM model in (4) and the MCA model in (5), respectively. In order to represent the typical noise scenarios given in [15], the mean power ratio of impulsive-to-background noises is set to be 30 dB in the GM model and 20 dB in the MCA model, respectively. The signal-to-noise ratio (SNR) is defined as $\text{SNR} = P_{\mathbf{s}}/P_{\mathbf{e}}$, where $P_{\mathbf{s}}$ is the power of the transmitted signal and $P_{\mathbf{e}}$ is the total noise power including the impulsive noise and background noise. The detailed simulation parameters are listed in Table 1.

Table 1: Parameters of simulations.

OFDM Carriers	FFT length $N = 128$, null tones $M = 56$, data tones $N - M = 72$
Modulation	4-QAM, 16-QAM
FEC Code	A rate-1/2 convolutional code
GM Model	$K = 3$, $p_k = \{0.9, 0.07, 0.03\}$, $\gamma_k = \{1, 100, 1000\}$
MCA model	$A = 0.1$, $\Gamma = 0.01$, and the first 10 terms are truncated.

In the same simulation environments, we compare the bit error rate (BER) performances between our proposed method and several available mitigation methods in the literature. In Figures 2–7, we identified the three SBL-based algorithms in [15], respectively, as their original notations: "SBL with null tones", "SBL with all tones", and "SBL with DF"; and the conventional OFDM system without impulsive noise mitigation as "No mitigation". For comparisons between nonparametric and parametric methods, we also present the results for the MMSE detectors with noise state information (NSI) in [12] which is identified as "MMSE with NSI". Note that the MMSE detector with NSI is optimal among the parametric methods [12].

5.1. Ideal Channel. Figures 2–5 compare the BER performances of all the above mitigation techniques for uncoded and coded systems using 4-QAM and 16-QAM, respectively. No result of the "SBL with DF" method is shown in Figures 2 and 4 since it is not applicable for uncoded systems.

We first analyze the results for the uncoded 4-QAM system in Figure 2. Obviously, our proposed "LP-All" and "ADMM-All" outperforms all the other methods except for the MMSE detector with NSI which appears the best in a lower SNR region. However, as SNR increases, our method becomes the most advantageous in moderate to high SNR region. When only the nondata tones are considered for impulsive noise estimation, the algorithm "LP-Null" and "ADMM-Null" achieve less SNR gains than the SBL algorithm with null tones under both impulsive noise models. Conversely, with all the tones being taken into account, the "LP-All" and "ADMM-All" exploiting the modulus of constellation points present advantages over the SBL algorithm with all tones, achieving an SNR gain more than 2 dB in the GM model or between 4 dB and 6 dB in the MCA model, respectively.

Then, we analyze the results presented in Figure 3 for the coded systems using 4-QAM. Again, our proposed method demonstrates a favorable capability of outperforming most of other algorithms in a similar tendency to that for the uncoded systems in Figure 2. Compared with the SBL with DF algorithm, our method presents a marginal performance loss in lower SNR region with GM impulsive noise. Conversely, in

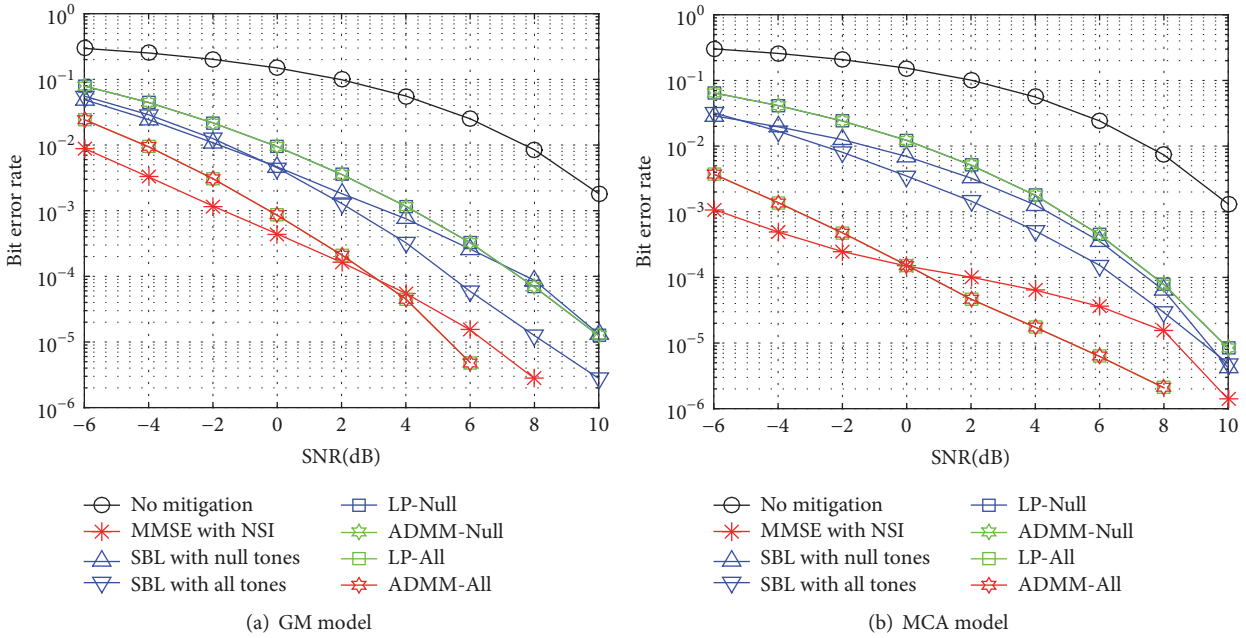

(a) GM model (b) MCA model

Figure 2: BER performance comparison for various mitigation methods in uncoded 4-QAM system.

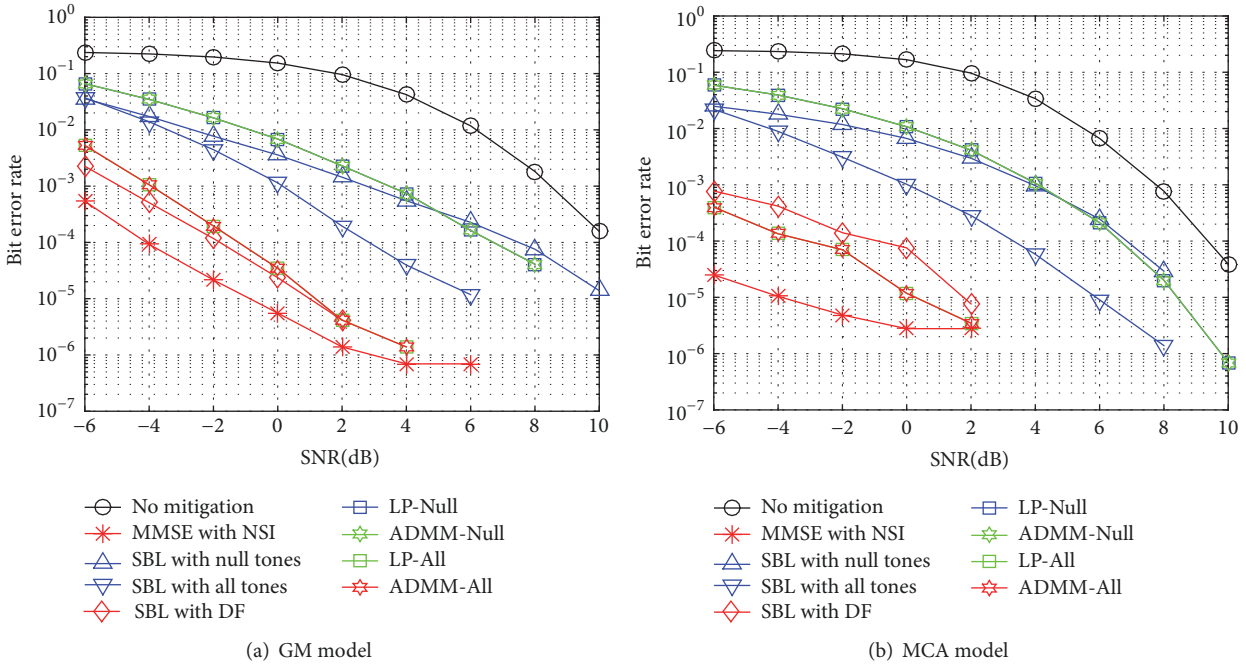

(a) GM model (b) MCA model

Figure 3: BER performance comparison for various mitigation methods in coded 4-QAM system.

the scenario of MCA, our method achieves a relatively larger SNR gain, where the SBL with DF algorithm no longer works as well as in GM since it needs to impose a priori information to the covariance matrix of impulsive noise [15].

From the simulation results for 16-QAM in Figures 4 and 5, it is observed that the BER performances of all the mitigation methods are degraded in both uncoded and coded cases. This can be explained in that the constellation points for high-order modulation become much tighter for transmit power given, and, hence, the detection of OFDM data symbols are more susceptible to the impulsive noise residual. As a consequence, over a wide range of SNR values, the MMSE with NSI becomes even worse than the SBL with null tones in the uncoded system and than the SBL with DF in the coded system, respectively. Moreover, the SBL with null tones becomes more effective than the SBL with all

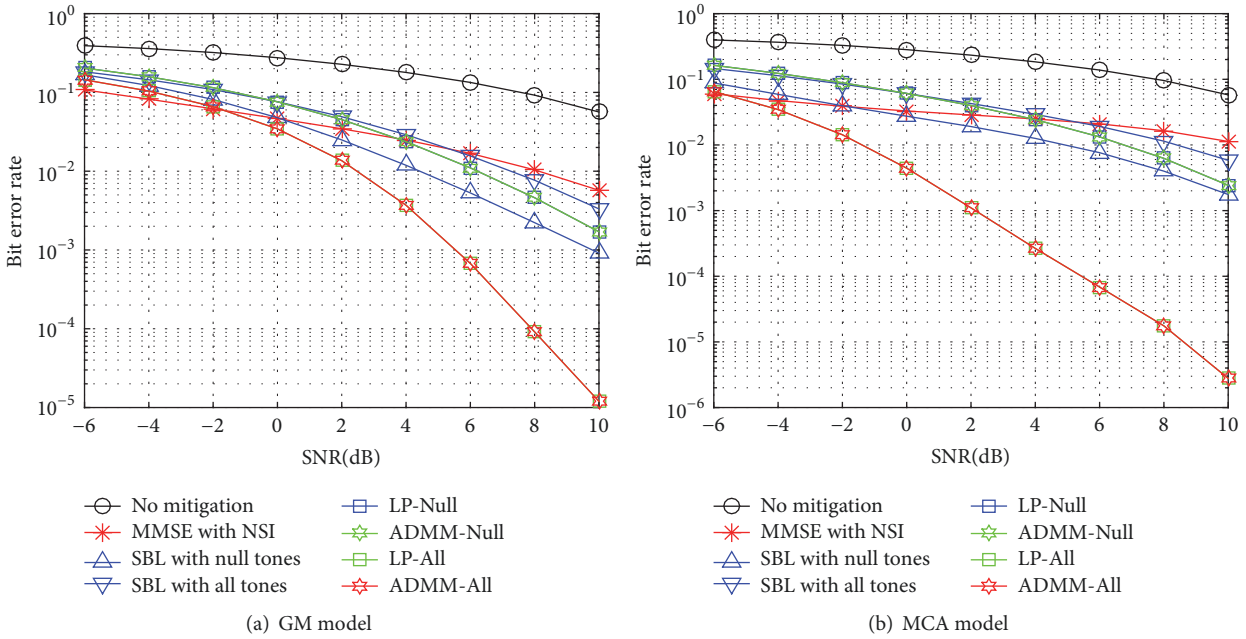

(a) GM model (b) MCA model

Figure 4: BER performance comparison for various mitigation methods in uncoded 16-QAM system.

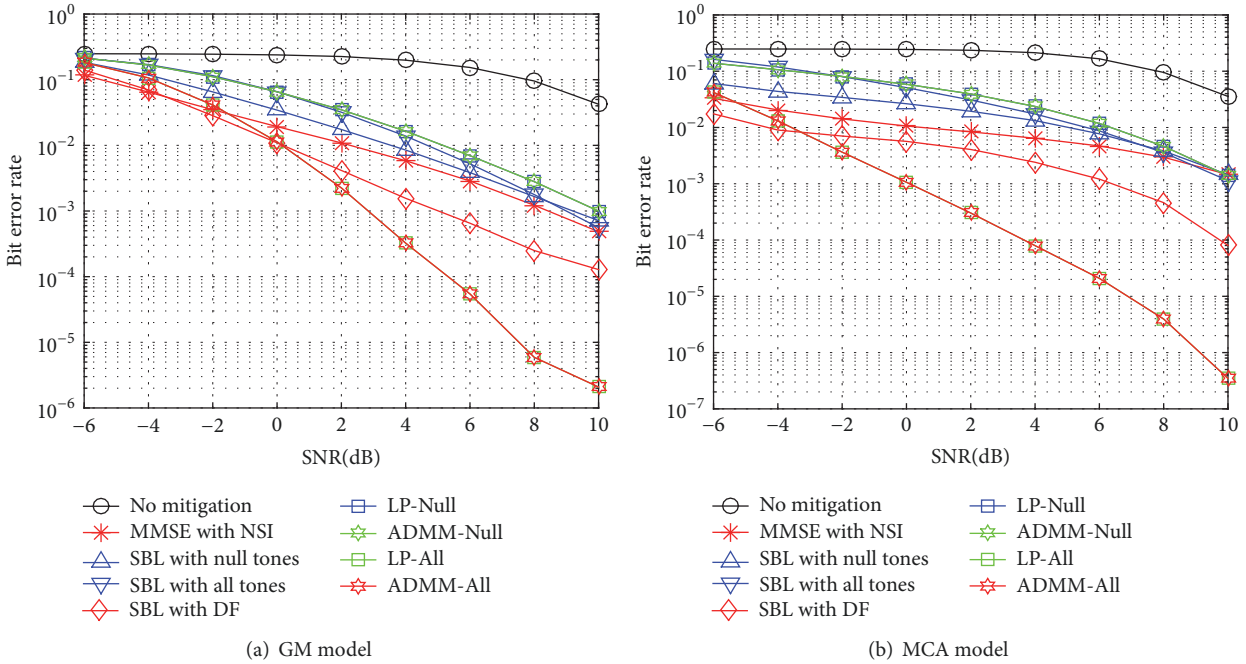

(a) GM model (b) MCA model

Figure 5: BER performance comparison for various mitigation methods in coded 16-QAM system.

tones. It is promising to observe that, in the 16-QAM systems, our method can obtain substantial performance gains over all other methods for moderate to high SNR values, and it becomes the best method for achieving the BERs below 10^{-2} for practical purposes.

5.2. PLC Channel. In this section, the 15-path multipath model is adopted as the PLC channel, parameters of which are the same as those listed in Table IV in [25]. The frequency range is 35~91 kHz, which is adopted by the NBPLC standard [19, 26]. Using the model, we can obtain the subcarrier gain, which are used as the diagonal elements of matrix in (11). At the receiver the zero-forcing equalizer is adopted to equalize the received symbols. As the PLC channel is deep fading channel, we set the SNR range is 0~20 dB. Figures 6 and 7 compare the BER performances of all the above mitigation techniques for uncoded and coded systems using 4-QAM, respectively.

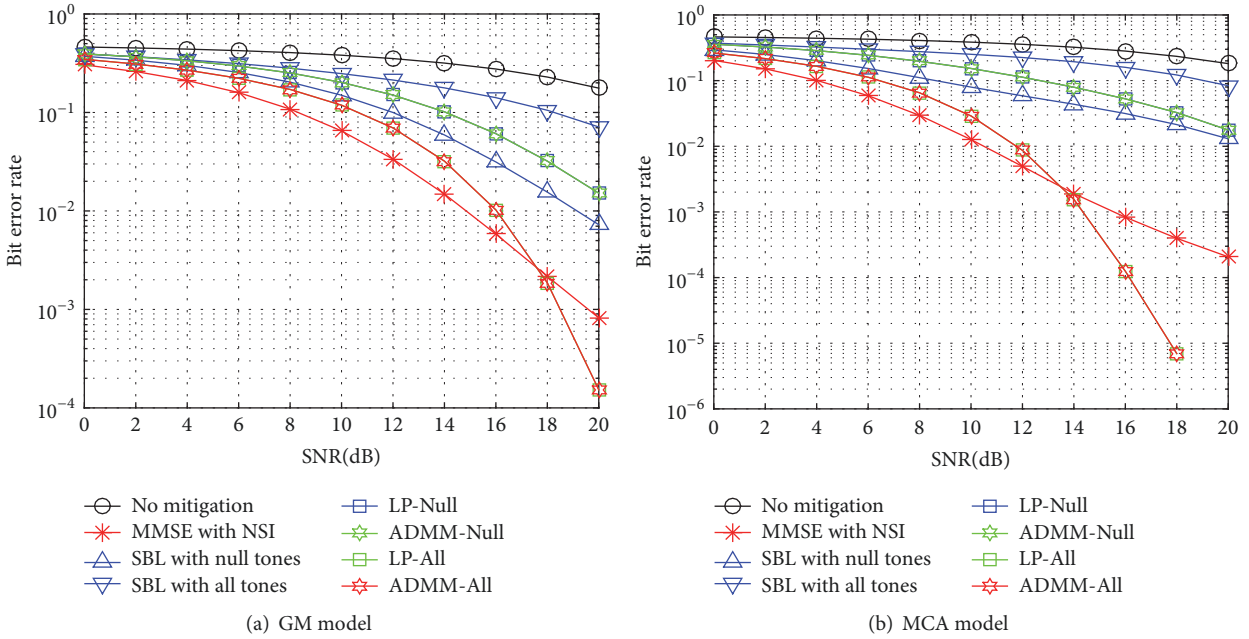

(a) GM model (b) MCA model

FIGURE 6: BER performance comparison for various mitigation methods in uncoded 4-QAM system. The PLC channel frequency response is known at the receiver.

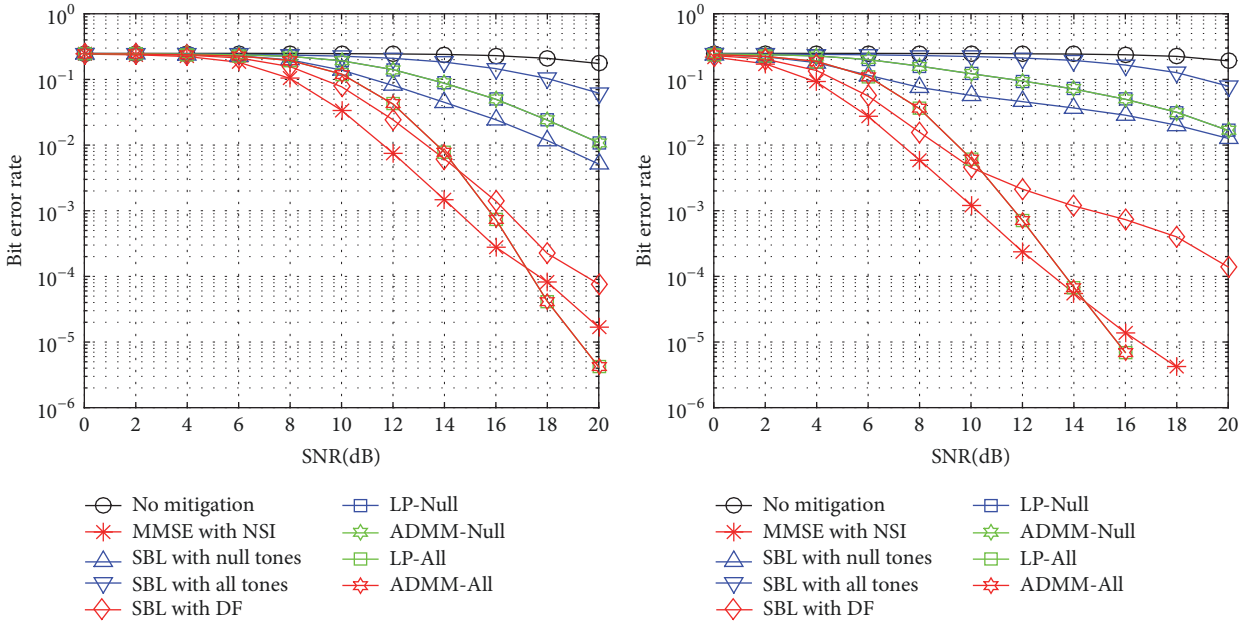

(a) GM model (b) MCA model

FIGURE 7: BER performance comparison for various mitigation methods in coded 4-QAM system. The PLC channel frequency response is known at the receiver.

We first analyze the result for the uncoded 4-QAM system in Figure 6. Obviously, our method outperforms all the other methods except for the MMSE detector with NSI which appears the best in the lower to moderate SNR region. However, as SNR increases, the "LP-All" and "ADMM-All" becomes the most advantageous in high SNR region. Moreover, the SBL with null tones and the CS algorithm "LP-Null" and "ADMM-Null" are more effective than the SBL with all tones.

Then, we analyze the results presented in Figure 7 for the coded systems using 4-QAM. Again, our proposed "LP-All" and "ADMM-All" demonstrate a favorable capability of

outperforming most of other algorithms in a similar tendency to that for the uncoded systems in Figure 6. Compared with the SBL with DF algorithm, our method presents a marginal performance loss in moderate SNR region. However, as SNR increases, our method achieves a relatively larger SNR gain.

6. Conclusion

In this paper, we have explored a nonparametric CS method for mitigating the asynchronous impulsive noise in OFDM-based PLC systems. The proposed method extends the conventional CS technique to exploit information with respect to all tones of OFDM symbol. Upon imposing detection constraints on the equalized symbols, the impulsive noise estimation has been formulated as a nonconvex optimization problem and then changed to be an LP problem with polynomial complexities. The ADMM framework is adopted to reduce the computation complexity. Simulation results have shown that the proposed method can achieve BER performance improvements at reduced computational complexities compared with the conventional methods. In particular, it provides a practical technique of asynchronous impulsive noise mitigation in PLC systems which employ high-order QAM for increasing the system throughput. It is worth mentioning that the proposed method can also be applied in the periodic impulsive noise mitigation when incorporating the time domain interleaving (TDI-OFDM) technique of [27].

Data Availability

The Matlab Source Code data used to support the findings of this study are available from the corresponding author upon request.

Conflicts of Interest

The authors declare that there are no conflicts of interest regarding the publication of this paper.

Acknowledgments

This work was supported in part by the National Natural Science Foundation of China under Grant no. 61571250, the Natural Science Foundation of Zhejiang Province under Grant no. LY18F010010, the Zhejiang Open Foundation of the Most Important Subjects under Grant no. XKXL1415, the Science Foundation of Zhejiang Business Technology Institute under Grant no. 2017Z01, the K. C. Wong Magna Fund in Ningbo University, and Key Laboratory of Mobile Internet Application Technology of Zhejiang Province.

References

[1] S. Galli, A. Scaglione, and Z. Wang, "For the grid and through the grid: the role of power line communications in the smart grid," *Proceedings of the IEEE*, vol. 99, no. 6, pp. 998–1027, 2011.

[2] Y. Yan, Y. Qian, H. Sharif, and D. Tipper, "A survey on smart grid communication infrastructures: Motivations, requirements and challenges," *IEEE Communications Surveys & Tutorials*, vol. 15, no. 1, pp. 5–20, 2013.

[3] G. Bumiller, L. Lampe, and H. Hrasnica, "Power line communication networks for large-scale control and automation systems," *IEEE Communications Magazine*, vol. 48, no. 4, pp. 106–113, 2010.

[4] M. Nassar, J. Lin, Y. Mortazavi, A. Dabak, I. H. Kim, and B. L. Evans, "Local utility power line communications in the 3–500 kHz band: channel impairments, noise, and standards," *IEEE Signal Processing Magazine*, vol. 29, no. 5, pp. 116–127, 2012.

[5] M. Ghosh, "Analysis of the effect of impulse noise on multicarrier and single carrier QAM systems," *IEEE Transactions on Communications*, vol. 44, no. 2, pp. 145–147, 1996.

[6] M. Zimmermann and K. Dostert, "Analysis and modeling of impulsive noise in broad-band powerline communications," *IEEE Transactions on Electromagnetic Compatibility*, vol. 44, no. 1, pp. 249–258, 2002.

[7] H. Meng, Y. L. Guan, and S. Chen, "Modeling and analysis of noise effects on broadband power-line communications," *IEEE Transactions on Power Delivery*, vol. 20, no. 2, pp. 630–637, 2005.

[8] S. V. Zhidkov, "Analysis and comparison of several simple impulsive noise mitigation schemes for OFDM receivers," *IEEE Transactions on Communications*, vol. 56, no. 1, pp. 5–9, 2008.

[9] F. H. Juwono, Q. Guo, D. Huang, and K. P. Wong, "Deep clipping for impulsive noise mitigation in OFDM-based power-line communications," *IEEE Transactions on Power Delivery*, vol. 29, no. 3, pp. 1335–1343, 2014.

[10] G. Ndo, P. Siohan, and M.-H. Hamon, "Adaptive noise mitigation in impulsive environment: Application to power-line communications," *IEEE Transactions on Power Delivery*, vol. 25, no. 2, pp. 647–656, 2010.

[11] E. Alsusa and K. M. Rabie, "Dynamic peak-based threshold estimation method for mitigating impulsive noise in power-line communication systems," *IEEE Transactions on Power Delivery*, vol. 28, no. 4, pp. 2201–2208, 2013.

[12] M. Nassar, *Graphical models and message passing receivers for interference limited communication systems [Ph.D. dissertation]*, University of Texas, Austin, TX, USA, 2013.

[13] G. Caire, T. Y. Al-Naffouri, and A. K. Narayanan, "Impulse noise cancellation in OFDM: an application of compressed sensing," in *Proceedings of the 2008 IEEE International Symposium on Information Theory - ISIT*, pp. 1293–1297, Toronto, ON, Canada, July 2008.

[14] L. Lampe, "Bursty impulse noise detection by compressed sensing," in *Proceedings of the 2011 IEEE International Symposium on Power Line Communications and Its Applications (ISPLC)*, pp. 29–34, Udine, Italy, April 2011.

[15] J. Lin, M. Nassar, and B. L. Evans, "Impulsive noise mitigation in powerline communications using sparse bayesian learning," *IEEE Journal on Selected Areas in Communications*, vol. 31, no. 7, pp. 1172–1183, 2013.

[16] T. Y. Al-Naffouri, A. A. Quadeer, and G. Caire, "Impulse noise estimation and removal for OFDM systems," *IEEE Transactions on Communications*, vol. 62, no. 3, pp. 976–989, 2014.

[17] M. Nassar, K. Gulati, Y. Mortazavi, and B. L. Evans, "Statistical Modeling of Asynchronous Impulsive Noise in Powerline Communication Networks," in *Proceedings of the 2011 IEEE Global Communications Conference (GLOBECOM 2011)*, pp. 1–6, Houston, TX, USA, December 2011.

[18] R. G. Baraniuk, "Compressive sensing," *IEEE Signal Processing Magazine*, vol. 24, no. 4, pp. 118–121, 2007.

[19] V. Oksman and J. Zhang, "G.HNEM: the new ITU-T standard on narrowband PLC technology," *IEEE Communications Magazine*, vol. 49, no. 12, pp. 36–44, 2011.

[20] N. D. Sidiropoulos and Z.-Q. Luo, "A semidefinite relaxation approach to MIMO detection for high-order QAM constellations," *IEEE Signal Processing Letters*, vol. 13, no. 9, pp. 525–528, 2006.

[21] CVX: Matlab software for disciplined convex programming. http://cvxr.com/cvx/.

[22] S. Boyd and L. Vandenberghe, *Convex Optimization*, Cambridge University Press, Cambridge, UK, 2004.

[23] S. Boyd, N. Parikh, E. Chu, B. Peleato, and J. Eckstein, "Distributed optimization and statistical learning via the alternating direction method of multipliers," *Foundations and Trends in Machine Learning*, vol. 3, no. 1, pp. 1–122, 2010.

[24] E. Ghadimi, A. Teixeira, I. Shames, and M. Johansson, "Optimal parameter selection for the alternating direction method of multipliers (ADMM): quadratic problems," *Institute of Electrical and Electronics Engineers Transactions on Automatic Control*, vol. 60, no. 3, pp. 644–658, 2015.

[25] M. Zimmermann and K. Dostert, "A multipath model for the powerline channel," *IEEE Transactions on Communications*, vol. 50, no. 4, pp. 553–559, 2002.

[26] M. Hoch, "Comparison of PLC G3 and PRIME," in *Proceedings of the 2011 IEEE International Symposium on Power Line Communications and Its Applications (ISPLC)*, pp. 165–169, Udine, Italy, April 2011.

[27] M. Mirahmadi, A. Al-Dweik, and A. Shami, "BER reduction of OFDM based broadband communication systems over multipath channels with impulsive noise," *IEEE Transactions on Communications*, vol. 61, no. 11, pp. 4602–4615, 2013.